

# **Dry deposition of reactive nitrogen to European ecosystems: a comparison of inferential models across the NitroEurope network – Supplementary Material**

**C. R. Flechard, E. Nemitz, R. I. Smith, D. Fowler, A. T. Vermeulen, A. Bleeker, J.W. Erisman, D. Simpson, L. Zhang, Y. S. Tang and M. A. Sutton**

## **A1 Introduction**

This supplement provides additional details concerning the implementation of four dry deposition (inferential) routines as part of the model inter-comparison at the ecosystem scale presented in the aforementioned article, with respect to ecosystem characteristics, micrometeorology and canopy wetness simulation.

## **A2 Canopy characteristics**

For the modelling of trace gas and particle deposition at national or regional scales, the inferential routines of the four models (i.e. CBED, CDRY, EMEP-03, IDEM) normally use either land use class (LUC)-specific, monthly default values, or phenological functions, for the key canopy characteristics (canopy height  $h_c$ , roughness length  $z_0$  and leaf area index LAI), since such data are not available at the ecosystem scale for every node of the grid domain nor for every day of the year. These default values or functions for each LUC logically differ between the four models since they were developed for different countries or climatic zones.

In this paper, however, the models are applied locally to a number of ecosystem study sites, rather than to a whole geographical domain. Measurements of  $h_c$  and of LAI were made as part of CarboEurope IP at most sites of the NitroEurope (NEU) inferential network (Table 1 of main paper). These measurements were carried out typically a few times during the growing season but the data capture was very uneven between sites. While the temporal (seasonal) variations were extremely well documented with very frequent (weekly) measurements at a few sites of the network, too few data were available at the majority of the

1 other sites to reliably interpolate over time, as required for input to deposition models. This is  
2 largely due to the fact that in many cases only the maximum LAI was recorded during the  
3 growing season, while the conditions at the start and end of the growing season can only be  
4 guessed. With several cuts per year in grasslands, or more than one crop per year in arable  
5 systems, the frequent measurements needed were not available for all sites. There was also the  
6 added problem that the NEU project (2006-2010) was shifted in time relative to CarboEurope  
7 IP (2004-2008), so that much of the LAI and  $h_c$  data collected as part of CarboEurope were  
8 not contemporaneous with the NEU trace gas and aerosol datasets (initiated in 2007). Another  
9 difficulty resides in the method or type of LAI measurement (single-sided, double-sided,  
10 projected, total) not being recorded, so that the available data may not be compatible with the  
11 input required for modelling.

12 Based on these considerations, model base runs in this study use model default values of LAI,  
13 combined with time-interpolated values of  $h_c$  derived from the available measured data  
14 ('ModLAI / MeasHc', see Table A2). The choice of model default LAI is primarily motivated  
15 by the potentially large error in measured LAI data, which may be considered just as  
16 uncertain as model default values. By contrast,  $h_c$  is a more easily measured and defined  
17 canopy characteristic, which can arguably be considered constant for forests over the time  
18 frame of CarboEurope and NEU. More importantly, the measurement heights for the sonic  
19 anemometers and for the DELTA gas and aerosol sampling apparatus were in practice set  
20 according to the true  $h_c$ . Thus the measured pollutant concentrations reflected vertical  
21 gradients and turbulent mixing conditions consistent with the real  $h_c$ , but not necessarily with  
22 a model default value.

23 Nevertheless, if the objective is to fully inter-compare models, rather than obtain the 'truest'  
24 model deposition estimates, one could argue that  $h_c$  and LAI descriptions in default lookup  
25 tables can be regarded as intrinsic model parameters, and should therefore both be used as  
26 inputs ('ModLAI / ModHc'). Conversely, using both sets of measured LAI and  $h_c$  as common  
27 inputs to the four models ('MeasLAI / MeasHc') could be defended as providing a better set-  
28 up for inter-comparing the models treatment of surface resistances, in which the confounding  
29 effects of surface roughness and area are removed. These alternative choices for the model  
30 inputs values of LAI and  $h_c$  are presented to assess the sensitivity of annual dry deposition  
31 fluxes (Figure A3). For the reconstruction of seasonal time series of daily  $h_c$  and LAI, the data  
32 were interpolated between consecutive measurements if their time resolution was sufficient;

1 alternatively, generic annual curves were computed on the basis of the standard EMEP-03  
 2 phenological functions (Simpson et al., 2003), then scaled using the measured minimum and  
 3 maximum values at each site.

4

### 5 **A3 Micrometeorological data**

6 Fundamental variables needed to compute the atmospheric resistances  $R_a$  and  $R_b$  include  $u_*$ ,  
 7 sensible heat flux  $H$ , and  $z_0$ . At 51 of the 55 sites of the NEU inferential network, long-term  
 8 eddy covariance (EC) measurements of  $\text{CO}_2$  and  $\text{H}_2\text{O}$  exchange were carried out within the  
 9 framework of CarboEurope IP (Aubinet et al., 2000), and thus actual in-situ measurements of  
 10  $u_*$  and  $H$  were available on a half-hourly basis and obtained courtesy of the CarboEurope-IP  
 11 database. For the 4 remaining non-CarboEurope IP sites (DE-Hoe, FI-Lom, NL-Spe, UA-Pet),  
 12 eddy covariance flux measurements were initiated as part of NitroEurope IP. In the base  
 13 model runs presented hereafter, all available measured (EC)  $u_*$  and  $H$  data were used by  
 14 default for the calculation of atmospheric resistances.

15 For cases when valid turbulence data from EC were not available due to instrument failure,  
 16 strong nocturnal atmospheric stability, small wind speeds or insufficient fetch (Aubinet et al.,  
 17 2000),  $u_*$  and  $H$  needed to be gap-filled from standard meteorological data (wind speed, net  
 18 radiation, temperature) measured at each site. This was done in a similar fashion to  
 19 meteorological sub-modules of regional chemical transport models (CTMs), which derive  
 20 their  $u_*$  from numerical weather prediction (NWP) model output data, such that (Thom,  
 21 1975):

$$22 \quad u_* = \frac{\kappa U(z_{ref} - d)}{\left[ \ln\left(\frac{z_{ref} - d}{z_0}\right) - \psi_M\left(\frac{z_{ref} - d}{L}\right) + \psi_M\left(\frac{z_0}{L}\right) \right]} \quad (\text{A1})$$

23 where  $z_0$  is roughness length and  $d$  is displacement height, both being dependent on  $h_c$ ,  $U$  is  
 24 wind speed,  $\kappa$  is von Karman's constant ( $= 0.41$ ),  $\psi_M$  is the integrated atmospheric stability  
 25 correction function for momentum, and  $L$  is the Obukhov stability length:

$$26 \quad L = -\frac{\rho_a \theta C_p u_*^3}{\kappa g H} \quad (\text{A2})$$

1 with  $\rho_a$  the density of dry air ( $\text{g m}^{-3}$ ),  $\theta$  the potential air temperature (K),  $C_p$  the specific heat  
2 capacity of air ( $= 1.005 \text{ J g}^{-1} \text{ K}^{-1}$ ) and  $g$  the gravitational acceleration ( $= 9.81 \text{ m s}^{-2}$ ) (Thom,  
3 1975). However, this also requires the knowledge of  $L$ , which is itself a function of both  $u_*$   
4 and  $H$  (Eq. A2). In the absence of valid micrometeorological measurements, a first and  
5 necessary step adopted here as in other models (e.g. Bassin et al., 2004) consists in a rough  
6 estimation of  $H$  assuming the closure of the surface energy balance and a partitioning of the  
7 available energy such that:

$$8 \quad H = R_n - \lambda E - G \quad (\text{A3})$$

9 Here  $G$  is the ground heat flux, and the latent heat flux  $\lambda E$  was estimated using the Penman-  
10 Monteith (P-M) equation, which may only be done in a first approximation assuming neutral  
11 stratification, since  $H$  and  $L$  are both unknown. As  $R_a$  and  $R_s$  are also needed, as rather poorly  
12 quantified drivers of evaporation, in the P-M equation, both estimates of  $\lambda E$  and  $H$  are  
13 necessarily quite uncertain, all the more as the surface energy closure assumption is often not  
14 confirmed in the field (e.g. Wohlfahrt et al., 2009). From the  $H$  estimate thus obtained, both  $u_*$   
15 and  $L$  are then calculated iteratively using Eqs. (A1) and (A2). The overall effect of the gap-  
16 filling procedure for  $H$  on annual  $N_r$  fluxes appears to be small, however, as the error in  $H$   
17 does not propagate very strongly into  $u_*$  (Bassin et al., 2004), and also because  
18 micrometeorological data gaps are by nature strongly correlated with periods of reduced wind  
19 speeds and suppressed turbulence, during which potential rates of tracer exchange are very  
20 small.

21

## 22 **A4 Surface potentials**

23 For the calculation of stomatal and non-stomatal resistances, and of the  $\text{NH}_3$  compensation  
24 point (Eqs. 3 to 10 in main Paper), values of the surface scalars temperature and relative  
25 humidity are required. From the viewpoint of a numerical weather prediction (NWP) model,  
26 ‘surface’ actually means anything between the measurement height ( $z_{\text{ref}}$ ) of a standard  
27 meteorological station within the surface layer, typically 2-3 m above ground or up to 10  
28 meters above tree tops in the case of a forest, up to 50-100 m. From a micrometeorological,  
29 field-scale point of view, ‘surface’ corresponds to the notional height  $z_s = d+z_0$ , ‘below’ the  
30 viscous sublayer, with  $z_0$  the roughness length for heat and trace gases (Monteith and  
31 Unsworth, 1990). There can be substantial differences between scalars at  $z_s$  and  $z_{\text{ref}}$ ,

1 depending on the intensity of turbulent mixing, canopy roughness, solar radiation and  
 2 atmospheric thermal stratification, especially over short vegetation. The temperature  
 3 difference between  $z_s$  and  $z_{ref}$  has a particularly strong impact on the calculation of the  
 4 stomatal compensation point ( $\chi_s$ ), which increases exponentially with temperature and doubles  
 5 approximately with every additional 4 – 5 K (Flechard and Fowler, 2008; Personne et al.,  
 6 2009), while for stomatal resistance the *vpd* stress factor  $f_e$  is best evaluated using relative  
 7 humidity at  $z_s$ .

8 By default in this paper, model base runs used ambient temperature and relative humidity data  
 9 as measured by meteorological stations at  $z_{ref}$ , a few m above vegetation, which is the closest  
 10 approximation to the outputs of NWP models that are normally used as inputs to CTMs. The  
 11 sensitivity of modelled fluxes to input  $T$  and  $RH$  was however tested in alternative model runs  
 12 by using the potentials at  $z_s$  rather than  $z_{ref}$  as input to the deposition routines (see ‘Surface  
 13 potentials’ model runs in Table A2 and Fig. A3). The  $z_s$  potentials were first computed from  
 14 measured micrometeorological fluxes of both sensible ( $H$ ) and latent heat ( $\lambda E$ ), following  
 15 (e.g. Monteith and Unsworth, 1990):

$$16 \quad T(z_0') = T(z_{ref} - d) + \frac{H}{\rho C_p} (R_a(z_{ref} - d) + R_{b,heat}) \quad (A4)$$

17 and

$$18 \quad e(z_0') = e(z_{ref} - d) + \frac{pE}{\rho \varepsilon} (R_a(z_{ref} - d) + R_{b,H_2O}) \quad (A5)$$

19 where  $e$  is water vapour pressure,  $p$  is atmospheric pressure,  $E$  is the water vapour flux and  $\varepsilon$   
 20 is the ratio of the molecular weight of water to the mean molecular weight of dry air (=  $18/29$ ), and the surface relative humidity is given by

$$22 \quad RH(z_0') = \frac{e(z_0')}{e_{sat}(T(z_0'))} \quad (A6)$$

23 where  $e_{sat}(T)$  is the saturation water vapour pressure at  $T$ .

24

## 25 **A5 Canopy wetness**

26 Surface wetness controls non-stomatal resistances for soluble trace gases in all four models,  
 27 particle rebound (EMEP-03, CDRY), and even stomatal ‘blocking’ (CDRY). Depending on

1 the process, chemical species and model considered, the wetness effect is either quantified by  
2 a continuous function of  $RH$  (e.g. Eq. 4-7 in main paper), or qualified by a binary (or boolean)  
3 indicator (wet =1 or true, dry =0 or false), with different surface resistances for the dry and  
4 wet cases. In the IDEM model, both a wetness indicator and the  $RH$  function (Eq. (7) in main  
5 paper) are used in turns for  $R_{ext}$  in the case of  $NH_3$ . Canopy wetness was actually monitored at  
6 a few sites of the NEU network (e.g. BE-Bra, CH-Oe1, NL-Spe, FR-Gri, UK-Amo) using  
7 surrogate sensors (e.g. Model 237 Leaf Wetness Sensor, Campbell Scientific, Logan, UT), but  
8 at most sites no measurements were available. For models in which a wetness boolean was  
9 required, this needed to be estimated from ancillary environmental data.

10 Although modelled  $R_w$ ,  $R_c$  and deposition flux are highly sensitive to wetness, canopy wetness  
11 is difficult to predict reliably. This is compounded by the fact that, although a leaf surface  
12 may appear dry to the eye or to surrogate wetness sensors, thin water films on microscopic  
13 scales, as demonstrated by leaf wetness/conductivity clips (Burkhardt and Eiden, 1994), still  
14 provide sinks for atmospheric gases, and thus a leaf surface might seldom be fully 'dry'.  
15 Various  $RH$  thresholds have been used as proxies to determine canopy wetness; van Jaarsveld  
16 (2004) determines a dry-wet switch point of 87% from surface wetness observations over  
17 mixed forest, while for grassland Wichink Kruit et al. (2008, 2010) suggest a smaller  
18 threshold at 71%. Both studies used ambient ( $z_{ref}$ )  $RH$  data, but it could be that the same  
19 analyses using  $RH(d+z_0')$  (see Section A4) might have yielded thresholds which were more  
20 similar to each other, given the larger vertical  $RH$  gradients over grassland than over forest.  
21 Some dry deposition models such as CDRY predict surface wetness semi-mechanistically and  
22 distinguish dew from rain, based on precipitation data and on night-time cloud cover and  $u_*$   
23 for dew formation. Other models either treat wetness as an input variable provided e.g. by  
24 NWP models, or use rule-of-thumb decisions based on ambient  $RH$  and precipitation. The  
25 CBED model does not actually require any wetness indicator to quantify the non-stomatal  
26 resistance for  $N_r$  gases.

27 Since the treatment of surface wetness prediction by the inferential models is rather crude and  
28 model-dependent, and since surface wetness can be regarded as an input variable to the  
29 models (rather than an output), it was preferred here to use a common wetness  
30 parameterisation to feed all four models. This suppresses the inter-model variability that  
31 would be caused by differing wetness schemes, and allows the model intercomparison to focus  
32 on discrepancies in surface resistances and fluxes. The approach used to simulate common

1 wetness data was based on the mechanistic, big leaf, surface wetness energy balance (SWEB)  
2 and canopy water budget model by Magarey et al. (2006). The SWEB model was originally  
3 designed for grapes but model canopy characteristics (LAI,  $h_c$ ) can be adjusted to deal with  
4 other crops and vegetation types. Inputs to the model are  $T$  and  $RH$  at the canopy height,  
5 precipitation, wind speed  $U$  measured at  $z_{ref}-d$  above the canopy and  $R_n$ . The model is  
6 dynamic, allowing surface water to accumulate up to the maximum storage capacity and to  
7 evaporate depending on meteorological conditions. The model therefore requires continuous  
8 input data, which were routinely available from meteorological stations at each site of the  
9 network. For cases when key meteorological variables were missing to run SWEB, but  
10 ambient  $RH$  was still available, canopy wetness was decided on the basis of a wet-dry  
11 threshold of 81%, which corresponds to the deliquescence point of ammonium sulphate  
12 (Flechard et al., 1999), although in reality deposited material on leaf surfaces is a mixture of  
13 various salts and organic aerosols. For the CDRY model, which requires a distinction of dew-  
14 from rain-wetted surfaces, the output of SWEB was split following CDRY decision rules.

15 The SWEB scheme (Magarey et al., 2006) was run systematically, regardless of the  
16 inferential model used, but the wetness output was slightly model-dependent, due to the  
17 differences in model LAI defaults. SWEB outputs are evaluated and compared in Fig. A2  
18 with measured data at five sites of the network, which were equipped with surrogate leaf  
19 wetness sensors (BE-Bra, CH-Oe1, FR-Gri, NL-Spe and UK-Amo). The data show the  
20 frequency (or probability) of wetness occurrence as a function of the time of day; there are  
21 strong seasonal variations that are driven by meteorological conditions, but for clarity the data  
22 are here averaged over the whole year. All sites describe a strong diurnal cycle, with the  
23 largest wetness frequency occurring toward late night/early morning, and the driest period  
24 occurring in mid to late afternoon, consistent with night-time dewfall and daytime  
25 evaporation of foliar wetness. The occurrence of rainfall may be considered to be randomly  
26 distributed through the day, having thus no effect on the shape of the diurnal cycle, though  
27 this is probably not be true for all sites.

28 Diurnal patterns and overall average wetness frequency are broadly consistent between  
29 observations and modelled values. The “wettest” canopy was found at the cut grassland site  
30 CH-Oe1 in both measurements and model simulations, with a night-time frequency of 90%  
31 and a daytime minimum of 40%. By contrast the other sites showed a night-time wetness  
32 probability of 50-80% and daytime minima of typically 20-30%. This was consistent with the

1 average annual rainfall being largest at CH-Oe1 (1200 mm). CH-Oe1 and FR-Gri had  
2 frequent dewfall due to frequent night-time inversions in semi-continental climates, while BE-  
3 Bra, NL-Spe and UK-AMo are windier sites in more oceanic conditions.

4 Differences between the various SWEB model runs at each site shown in Fig. A2 can  
5 essentially be ascribed to the canopy-scale, leaf surface wetness storage capacity, and  
6 consequently the different average leaf wetness durations, which are driven by different LAI  
7 defaults from each model. For example at the arable site of FR-Gri, the model run using  
8 EMEP-03 LAI defaults provided much smaller wetness frequencies than the other models,  
9 which was consistent with a much smaller mean annual LAI in EMEP-03 (0.42) than in  
10 CBED (1.35), CDRY (1.22) and IDEM (1.72). SWEB was also run for comparison using  
11 estimates of LAI provided at each site. At BE-Bra, CH-Oe1 and FR-Gri this did not  
12 significantly improve nor lessen SWEB performance, as compared with observations, but at  
13 NL-Spe and UK-AMo there was a noticeable improvement for night-time conditions, where  
14 observations apparently indicated much less frequent wetness occurrences than the canopy  
15 water budget approach.

16 It should be noted that “observed” wetness measurements can have significant uncertainties,  
17 and for example the small wetness values seen at night-time at the blanket bog site UK-AMo  
18 seem somewhat surprising (one would expect almost 100% humidity near the surface at night  
19 at such sites, which ought to cause wetness), but the representativity of, and the potential  
20 errors in, wetness measurements made using generally only one surrogate sensor cannot be  
21 assessed here and have been treated elsewhere (e.g. Wichink Kruit et al., 2008). The lack of  
22 spatial or vertical resolution in such data and the different behaviours of wetness sensors and  
23 leaves or needles with respect to water evaporation, condensation and to particle deposition,  
24 which favours condensation at smaller *RH* (Burkhardt and Eiden, 1994), might explain some  
25 of the discrepancies observed between measurements and models. On the other hand, any  
26 surface wetness and energy balance approach will suffer shortcomings and may perform  
27 better for certain types of vegetation than others. It is perhaps not surprising that the SWEB  
28 model by Magarey et al. (2006), having been developed for agricultural vegetation, seemed to  
29 give best results over grass at CH-Oe1 and cropland at FR-Gri, but in forests (BE-Bra, NL-  
30 Spe in Fig. A2) big leaf limitations may be significant. More validation data are required, but  
31 based on the few sites where a comparison was performed (Fig. A2), the SWEB approach  
32 may be considered robust and valid for the purposes of inferential modelling.



1

2 **A6 References**

- 3 Aubinet, M., Grelle, A., Ibrom, A., Rannik, U., Moncrieff, J., Foken, T., Kowalski, A.S.,  
4 Martin, P.H., Berbigier, P., Bernhofer, Ch., Clement, R., Elbers, J., Granier, A., Grünwald, T.,  
5 Morgenstern, K., Pilegaard, K., Rebmann, C., Snijders, W., Valentini, R. and Vesala, T.:  
6 Estimates of the annual net carbon and water exchange of forests: the EUROFLUX  
7 methodology, *Adv. Ecol. Res.*, 30, 113–171, 2000.
- 8 Bassin, S., Calanca, P., Weidinger, T., Gerosa, G. and Fuhrer, J.: Modelling seasonal ozone  
9 fluxes to grassland and wheat: model improvement, testing, and application, *Atmos. Environ.*,  
10 38, 2349-2359, 2004.
- 11 Burkhardt, J. and Eiden, R.: Thin water films on coniferous needles, *Atmos. Environ.*, 28,  
12 2001-2011, 1994.
- 13 Flechard, C.R., Fowler, D., Sutton, M.A., and Cape, J.N.: A dynamic chemical model of bi-  
14 directional ammonia exchange between semi-natural vegetation and the atmosphere, *Q. J.*  
15 *Roy. Meteor. Soc.*, 125, 2611-2641, 1999.
- 16 Flechard, C.R. and Fowler, D.: Effects of Changing Temperature on Leaf Surface Water-Film  
17 Chemistry and Trace Gas Exchange Processes over Terrestrial Vegetation, in: *The Impact of*  
18 *Climate Change on Air Quality, The 4th ACCENT Barnsdale Expert Workshop*, Editors: P.  
19 Builtjes, D. Fowler, J. Feichter, A. Lewis, P. Monks and P. Borrell, ACCENT Secretariat,  
20 Urbino, 155–161, 2008.
- 21 Magarey, R.D., Russo, J.M. and Seem, R.C.: Simulation of surface wetness with a water  
22 budget and energy balance approach, *Agr. Forest Meteorol.*, 139, 373–381, 2006.
- 23 Monteith, J.L. and Unsworth, M.H.: *Principles of Environmental Physics*, 2nd edition.  
24 Edward Arnold, London. 291 pp, 1990.
- 25 Personne, E., Loubet, B., Herrmann, B., Mattsson, M., Schjoerring, J.K., Nemitz, E., Sutton,  
26 M.A. and Cellier, P.: SURFATM-NH<sub>3</sub> : a model combining the surface energy balance and  
27 bi-directional exchanges of ammonia applied at the field scale, *Biogeosciences*, 6, 1371–  
28 1388, 2009.
- 29 Simpson, D., Fagerli, H., Jonson, J.E., Tsyro, S., Wind, P. and Tuovinen, J.-P.:  
30 Transboundary Acidification, Eutrophication and Ground Level Ozone in Europe. Part I:

- 1 Unified EMEP Model Description, EMEP Status Report 2003, ISSN 0806-4520, Det  
2 Meteorologisk Institutt, Oslo, 2003.
- 3 Thom, A.S.: Momentum, mass and heat exchange of plant communities. In: Vegetation and  
4 the atmosphere, vol. 1 (Ed: J.L. Monteith), pp 57-109. Academic Press, London, 1975.
- 5 van Jaarsveld J.A.: The Operational Priority Substances model: Description and validation of  
6 OPS-Pro 4.1, RIVM report 500045001/2004, 156 pp., Bilthoven, The Netherlands, 2004.
- 7 Wichink Kruit, R.J., Jacobs, A.F.G. and Holtslag, A.A.M.: Measurements and estimates of  
8 leaf wetness over agricultural grassland for dry deposition modelling of trace gases, Atmos.  
9 Environ., 42, 5304-5316, 2008.
- 10 Wichink Kruit, R.J., van Pul, W.A.J., Sauter, F.J., van den Broek, M., Nemitz, E., Sutton,  
11 M.A., Krol, M. and Holtslag, A.A.M.: Modelling the surface-atmosphere exchange of  
12 ammonia, Atmos. Environ., 44 (7), 945-957, 2010.
- 13 Wohlfahrt, G., Haslwanter, A., Hörtnagl, L., Jasoni, R.L., Fenstermaker, L.F., Arnone, J.A.  
14 and Hammerle, A.: On the consequences of the energy imbalance for calculating surface  
15 conductance to water vapour, Agr. Forest Meteor., 149, 1556-1559, 2009.
- 16

1 Table A1. Selected references for the measurement sites

Site Code	Site Name	Authors	Year	Journal	Vol.	Pages	
BE-Bra	Brasschaat	Neiryneck et al.	2005	Atmos. Environ.	39	5013-5024	
BE-Vie	Vielsalm	Heinesch et al.	2007	Boundary Layer Meteorol.	122	457-478	
CH-Lae	Laegeren	Ruehr et al.	2010	Biogeochemistry	98	153-170	
CZ-BK1	Bily Kriz	Sedlak et al.	2010	Agric. Forest Meteorol.	150	736-744	
DE-Hai	Hainich	Knohl et al.	2003	Agric. Forest Meteorol.	118	151-167	
DE-Hoe	Höglwald	Kreutzer et al.	2009	Plant Biol.	11	643-649	
DE-Tha	Tharandt	Grünwald and Bernhofer	2007	Tellus	59B	387-396	
DE-Wet	Wetzstein	Anthoni et al.	2004	Glob. Change Biol.	10	2005-2019	
DK-Sor	Soroe	Pilegaard et al.	2003	Boreal Environ. Res.	8	315-333	
ES-ES1	El Saler	Sanz et al.	2002	Environm. Pollution	118	259-272	
ES-LMa	Las Majadas	Casals et al.	2009	Soil Biol. Biochem.	41	1915-1922	
FI-Hyy	Hyytiälä	Vesala et al.	2005	Glob. Biogeochem. Cycles	19	n° GB2001	
FI-Sod	Sodankylä	Thum et al.	2008	Biogeosciences	5	1625-1639	
FR-Fon	Fontainbleau	Davi et al.	2006	Agric. Forest Meteorol.	139	269-287	
FR-Hes	Hesse	Granier et al.	2008	Ann. For. Sci.	64	n° 704	
FR-LBr	Le Bray	Rivalland et al.	2005	Ann. Geophysicae	23	291-304	
FR-Pue	Puechabon	Allard et al.	2008	Glob. Change Biol.	14	714-725	
IT-Col	Collelongo	Scartazza et al.	2004	Oecologia	140	340-351	
IT-Ren	Renon	Marcolla et al.	2005	Agric. Forest Meteorol.	130	193-206	
IT-Ro2	Roccarespampani	Tedeschi et al.	2006	Glob. Change Biol.	12	110-121	
IT-SRo	San Rossore	Chiesi et al.	2005	Agric. Forest Meteorol.	135	22-34	
NL-Loo	Loobos	Dolman et al.	2002	Agric. Forest Meteorol.	111	157-170	
NL-Spe	Speulderbos	Erisman et al.	1999	Water, Air, and Soil Pollution	109	237-262	
PT-Esp	Espirra	Pereira et al.	2007	Biogeosciences	4	791-802	
PT-Mi1	Mitra II (Evora)	Pereira et al.	2007	Biogeosciences	4	791-802	
RU-Fyo	Fyodorovskoye	Ramonet et al.	2002	Tellus	54B	713-734	
SE-Nor	Norunda	Grelle et al.	1999	Agric. Forest Meteorol.	98-99	563-578	
SE-Sk2	Skyttorp	Lindroth et al.	2008	Tellus	60B	129-142	
UK-Gri	Griffin	Clement et al.	2003	Scottish Forestry	57	5-10	
DE-Meh	Mehrstedt	Don et al.	2009	Glob. Change Biol.	15	1990-2002	
ES-VDA	Vall d'Alinyà	Sebastià	2007	J. App. Ecology	44	158-167	
FI-Lom	Lompolojännkä	Aurela et al.	2009	Boreal Environ. Res.	14	699-710	
HU-Bug	Bugac	Nagy et al.	2007	Agric. Ecosys. Environ.	121	21-29	
IT-Amp	Amplero	Gavrichkova et al.	2010	Agric. Ecosys. Environ.	136	87-96	
IT-MBo	Monte Bondone	Vescovo and Gianelle	2006	Agric. Ecosys. Environ.	115	141-149	
NL-Hor	Horstermeer	Hendriks et al.	2007	Biogeosciences	4	411-424	
PL-wet	POLWET						
UK-AMo	Auchencorth Moss	Flechard et al.	1998	Quart. J. Roy. Meteorol. Soc.	124	733-757	
CH-Oe1	Oensingen	Flechard et al.	2005	Glob. Change Biol.	11	2114-2127	
DE-Gri	Grillenbug	Tittebrand et al.	2009	Theor. Appl. Climatol.	98	171-186	
DK-Lva	Rimi	Gryning et al.	2009	Boreal Environ. Res.	14	204-212	
FR-Lq2	Laqueuille	Allard et al.	2007	Agric. Ecosys. Environ.	121	47-58	
IE-Ca2	Carlow	Abdalla et al.	2009	Geoderma	151	327-337	
IE-Dri	Dripsey	Byrne et al.	2005	Agric. Forest Meteorol.	135	82-92	
NL-Ca1	Cabauw	Jacobs et al.	2007	Biogeosciences	4	803-816	
UK-EBu	Easter Bush	Milford et al.	2001	Water Air Soil Pollution Focus	1	167-176	
BE-Lon	Lonzee	Moureaux et al.	2006	Agric. Forest Meteorol.	139	25-39	
DE-Geb	Gebesee	Anthoni et al.	2004	Agric. Forest Meteorol.	121	55-67	
DE-Kli	Klingenberg	Tittebrand et al.	2009	Theor. Appl. Climatol.	98	171-186	
DK-Ris	Risbyholm	Houborg and Soegaard	2004	Remote Sensing Environ.	93	150-167	
FR-Gri	Grignon	Lamaud et al.	2009	Agric. Forest Meteorol.	149	1385-1396	
IT-BCi	Borgo Cioffi	Vitale et al.	2009	Acta Physiol. Plant.	31	331-341	
IT-Cas	Castellaro	Rossini et al.	2010	Agric. Forest Meteorol.	150	1283-1296	
UA-Pet	Petrodolinskoye	Medinets et al.	2009	Ecology of the cities and recreation zones, ISBN 978-966-8885-28-0 (in russian)		103-107	
UK-ESa	East Saltoun	<a href="http://www.geos.ed.ac.uk/abs/research/micromet/Current/esaltoun/">http://www.geos.ed.ac.uk/abs/research/micromet/Current/esaltoun/</a>					

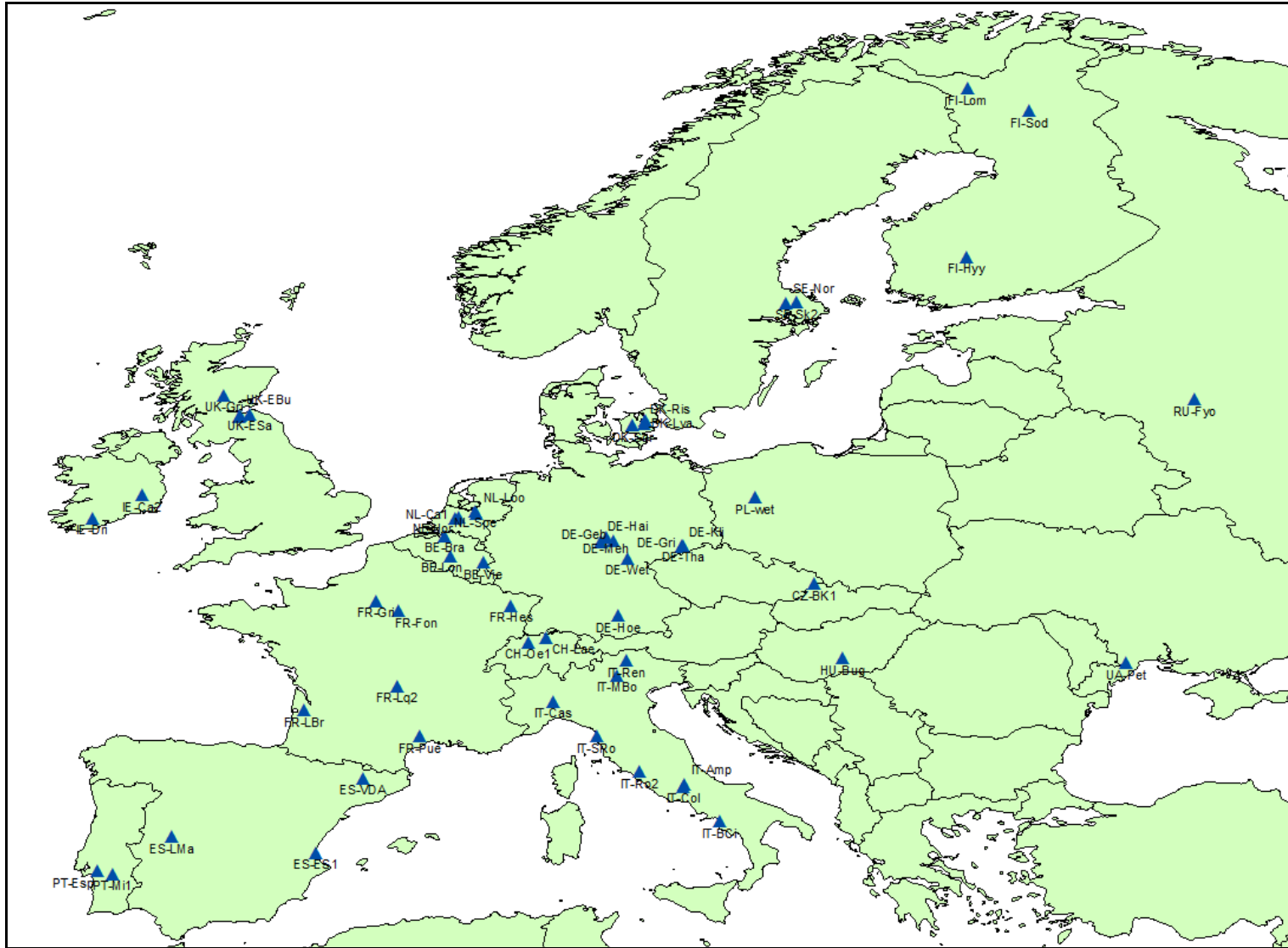
2

3

4

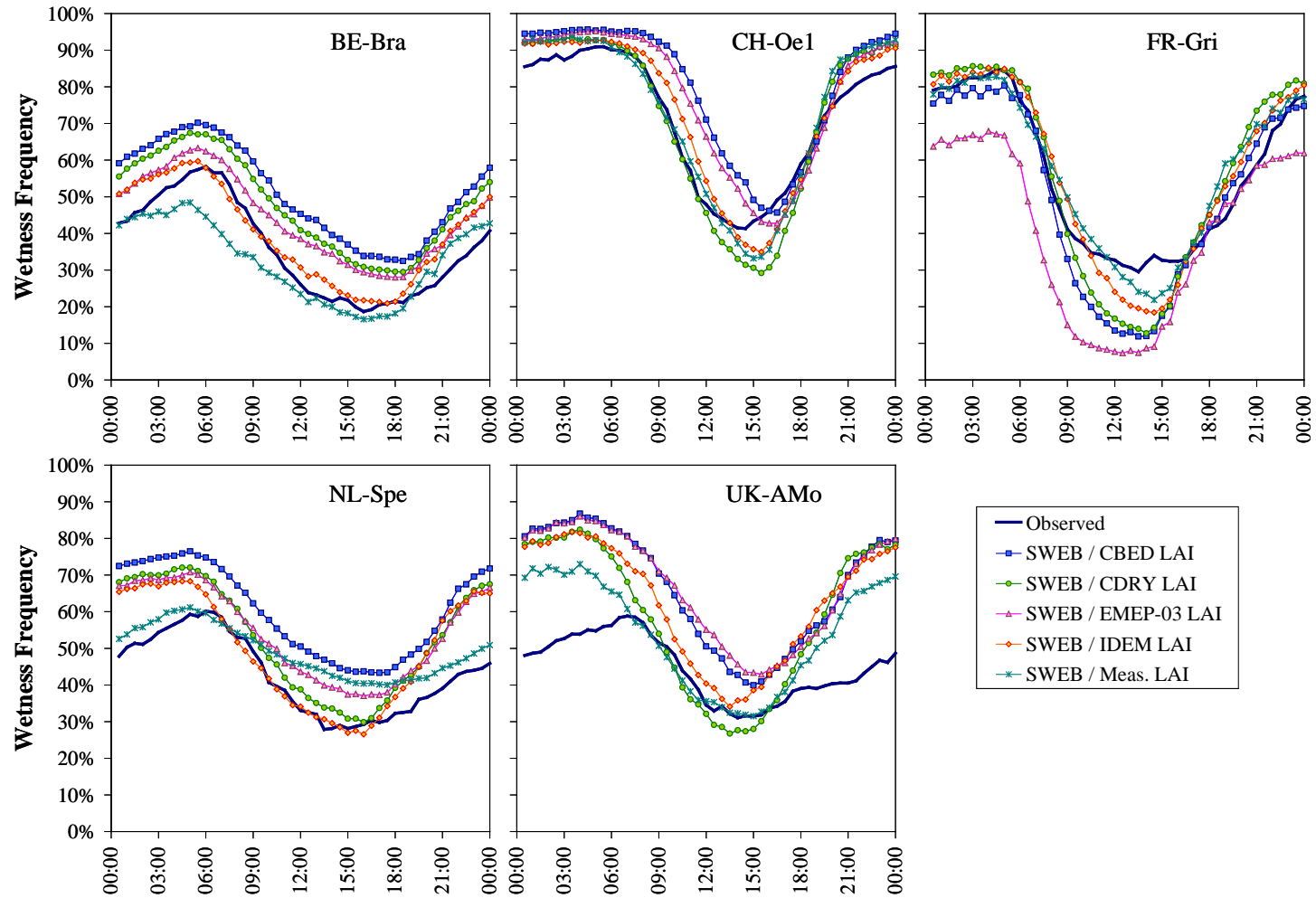
1 Table A2. Summary of input data used in model base runs and tested for sensitivity in  
 2 alternative runs.

Model runs	LAI	$h_c$	Temperature	Relative humidity	Stability corrections
<b>Base Runs</b>					
<i>ModLAI / MeasHc</i>	Model default	Measured	Ambient	Ambient	Yes
<b>Alternative Runs</b>					
<i>ModLAI / ModHc</i>	Model default	Model default	Ambient	Ambient	Yes
<i>MeasLAI / MeasHc</i>	Measured	Measured	Ambient	Ambient	Yes
<i>Surface Potentials</i>	Model default	Measured	$z_0'$	$z_0'$	Yes
<i>No stability correction (CBED )</i>	Model default	Measured	Ambient	Ambient	No

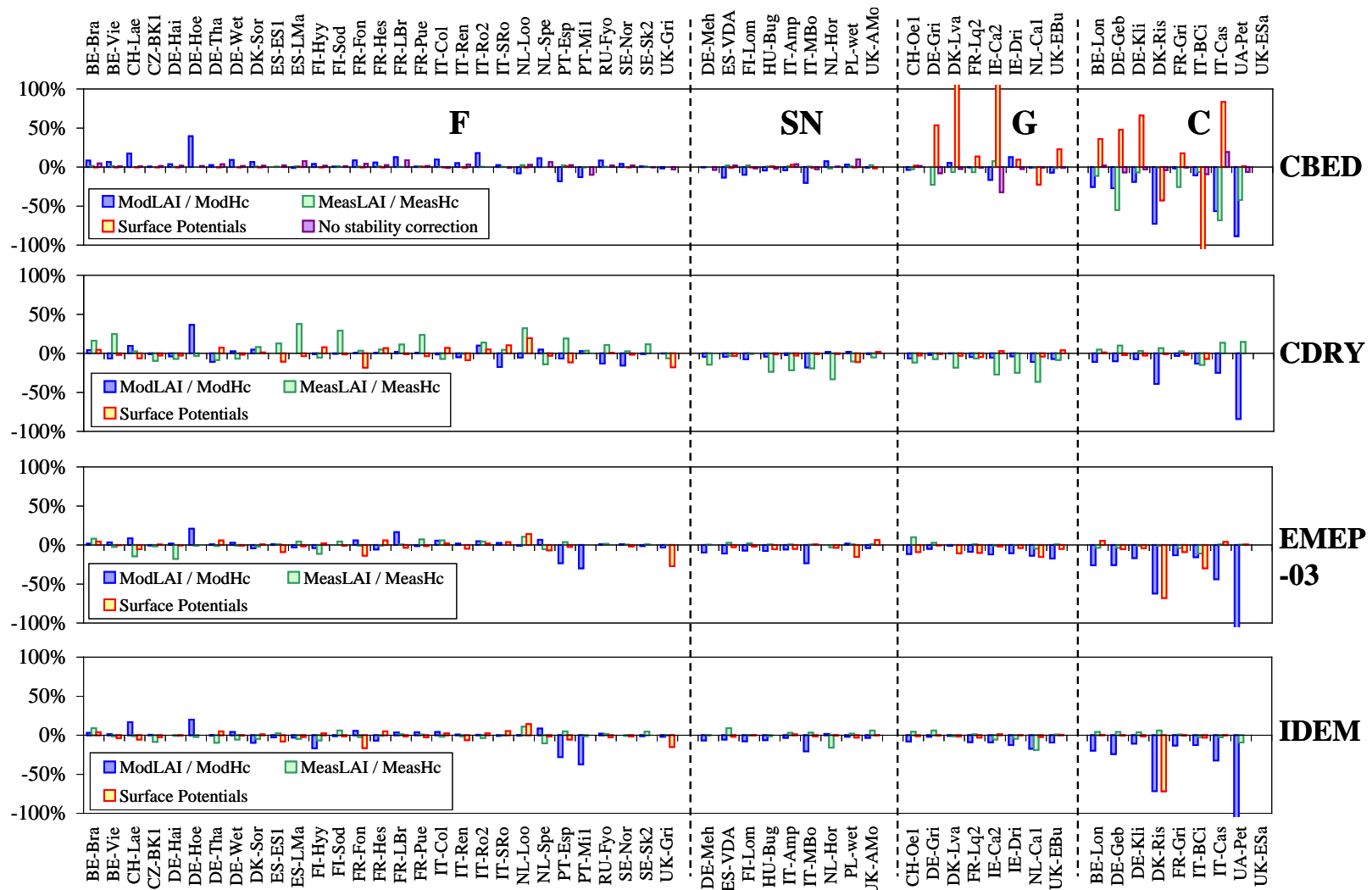


1  
2  
3

Figure A1. Geographical locations of NITROEUROPE inferential network sampling sites.



1  
 2 Figure A2. Comparison of observed and modelled annual diurnal cycles of canopy wetness frequency at five sites of the inferential network.  
 3 Modelled values were obtained by running the surface wetness energy balance model (SWEB, Magarey *et al.*, 2006), using as input either the  
 4 model default LAI values for each of CBED, CDRY, EMEP-03 and IDEM, or using the measured LAI.  
 5



1  
 2 Figure A3. Sensitivity of modelled annual  $N_r$  dry deposition fluxes to the choice of input data for LAI,  $h_c$  (measured vs model default), to the  
 3 use of temperature and relative humidity at the surface ( $d+z_0'$ ) rather than ambient, and to the non-implementation of stability corrections  
 4 (CBED only). The percentage differences are expressed relative to the model base runs as detailed in Table A2, with a negative number  
 5 indicating larger dry deposition (or smaller emission), and a positive number indicating smaller dry deposition (larger emission).